Received: 16 December 2024 | Revised: 27 September 2025 | Accepted: 7 November 2025

DOI: 10.1002/ppp3.70138

RESEARCH ARTICLE

Plants People Planet PPF Open Access

Made in the shade: Leaf responses of native wildflowers to single-axis photovoltaic solar energy

Yudi Li[1,2] | Troy Magney[3] | Alona Armstrong[4,5] | Rebecca R. Hernandez[1,2,4,5]

[1]Wild Energy Center, University of California - Davis, Davis, California, USA

[2]Department of Land, Air and Water Resources, University of California - Davis, Davis, California, USA

[3]W.A. Franke College of Forestry and Conservation, University of Montana, Missoula, Montana, USA

[4]Lancaster Environment Centre, Lancaster University, Lancaster, UK

[5]Energy Lancaster, Lancaster University, Lancaster, UK

Correspondence
Yudi Li, Wild Energy Center, Energy and Efficiency Institute, University of California - Davis, Davis, CA 95616, USA.
Email: evoli@ucdavis.edu

Funding information
This study was supported by Electric Power Research Institute (EPRI) (Award/Grant Number: 10014423). Additional funding for RRH and YL was provided by the Agricultural Experiment Station Hatch projects CA-R-A-6689-H and CA-D-LAW-2352-H and the Department of Land, Air, and Water Resources at the University of California, Davis.

Societal Impact Statement

As solar energy expands globally, balancing renewable power generation with biodiversity and ecosystem health has become an urgent challenge. This study investigated how native wildflowers respond at the leaf level to the unique microclimates created by rotating solar panels in California's Central Valley. We found that panels reduced light and water stress while prompting leaf area expansion, particularly in shade-tolerant species. These insights reveal the potential benefits of partial shade in semi-arid regions, highlight the plasticity of native wildflowers to altered microenvironments, and underscore the importance of strategic species selection to advance ecological restoration efforts at large solar farms.

Summary

- Ground-mounted photovoltaic solar energy facilities (GPVs), especially those equipped with tracking systems, are rapidly expanding worldwide, raising growing concerns about land-use conflict and environmental degradation. Co-locating GPVs with ecological restoration is gaining popularity, representing a promising pathway towards sustainable renewable energy development. Yet, the physiological and morphological responses of incorporated plants to GPVs remain understudied, hindering strategic planning and the effectiveness of revegetation.
- A combination of rapid, minimally invasive methods was employed in both field and laboratory settings to investigate leaf acclimations over a 12-month period in two native perennial wildflowers—differing in lifeform and shade tolerance—that were sown and successfully established after a full growing season at a single-axis tracking GPV site in the semi-arid Central Valley of California.
- Shadow cast by PV infrastructure alleviated excess light and water stresses, promoted leaf area expansion, and suppressed polyphenol accumulation in both species. Some responses fluctuated diurnally with panel rotation, while seasonal variations were primarily governed by ontogenetic development. Both perennials thrived within the array footprint, though *Phacelia californica* exhibited greater light-use efficiency, transpiration rate, and chlorophyll content compared with the

sun-loving competitor *Grindelia camporum*, which showed notable plasticity but reduced stomatal conductance, indicative of a more conservative water-use scheme.

- By revealing species-specific, spatiotemporal patterns of leaf acclimation in two native wildflowers, this study highlights how fine-scale microclimatic variability—driven by single-axis tracking GPVs—modulates leaf physiological and morphological responses, thereby informing strategies to align renewable energy production with biodiversity net gain and ecosystem service delivery.

KEYWORDS
biodiversity, ecophysiology, ecovoltaic, microclimate, restoration, solar photovoltaic, vegetation, wildflower

1 | INTRODUCTION

The global expansion of large, ground-mounted photovoltaic solar energy facilities (GPVs) is primarily driven by rising electricity demand and the urgent need to mitigate climate change (IEA, 2024). However, the operation of PV panels alters site microclimates by casting shade, redistributing precipitation, emitting heat, and obstructing airflow (Armstrong et al., 2016; Barron-Gafford et al., 2019; Hassanpour Adeh et al., 2018; Li et al., 2025; Wu et al., 2022). These shifts can modify vegetation composition, structure, demography, and phenology (Lambert et al., 2021; Liu et al., 2019; Tanner et al., 2020, 2021; Uldrijan et al., 2021; Uldrijan et al., 2022 & Walston et al., 2021). In the face of dual climate and biodiversity crises, ecovoltaics—the co-location of PV solar energy generation with ecological restoration and management—is a promising, albeit understudied strategy for mitigating climate change and bolstering ecosystem services (Fernández-Bou & Yang, 2024; Hernandez et al., 2024; Sturchio & Knapp, 2023; Tölgyesi et al., 2023). Yet, the extent to which vegetation responds to solar infrastructure and operation at physiological, morphological, and biochemical levels remains poorly understood, limiting our ability to predict and maximize restoration outcomes, such as the successful establishment of native grasslands or prairies at GPVs (Furtak & Nosalewicz, 2022; Mathur et al., 2018; Sturchio et al., 2024).

Leaves, as the primary organs for photosynthesis and transpiration, are essential to plant growth and development (Tsukaya, 2013; Wang et al., 2021). Shade can enhance photochemical efficiency of Photosystem II (Φ_{PSII}) to sustain photosynthetic capacity while diminishing transpiration by curbing stomatal conductance (g_{sw}) under excess light or heat (Idris et al., 2018; Urban et al., 2017). Larger specific leaf area (SLA), width-to-length ratio, and chlorophyll content—especially chlorophyll b, which is more susceptible to photodamage than chlorophyll a—are also typically observed in shaded leaves (relative to sun leaves) to compensate for lower incident radiation, along with reduced protective pigment pools of carotenoids and polyphenols (Carins Murphy et al., 2012; Dubey, 2018; Lichtenthaler et al., 2007). Acclimation to shade in leaves may also be evident using high-throughput approaches in (i) reflectance spectra, such as greater normalized difference vegetation index (NDVI) and more negative photochemical reflectance index (PRI), suggesting enhanced green leaf area and light-use efficiency, respectively (Gamon et al., 2015; Gerhards et al., 2016); and, (ii) thermal performance metrics, like lower crop water stress index (CWSI)—inversely associated with leaf water potential—and higher stomatal conductance index (Ig) that is linearly correlated with g_{sw} (Craparo et al., 2017; Maes & Steppe, 2012). Overall, such plasticity may enable plants to optimize their energy-water balance in novel microenvironments created within GPV-impacted landscapes.

Effects from fixed-tilt PV panels have been shown to increase chlorophylls while reducing anthocyanins and flavanols in a sun-loving bromegrass in France (Lambert et al., 2022) and facilitate chlorophyll, starch, and nutrient accumulation of two desert shrubs in Nevada, USA, at the expense of smaller canopy volumes and seed yields (Wynne-Sison et al., 2023). In Italy, negative effects of excessive mid-day irradiance on photosynthesis and drought susceptibility in grapevines were attenuated from GPV-driven shading (Ferrara et al., 2023). Crops such as wheat, lettuce, and pepper cultivated beneath elevated PVs demonstrated increased leaf length, width, temperature, g_{sw}, and yield compared with those in open-field conditions (Barron-Gafford et al., 2019; Dupraz et al., 2011; Marrou et al., 2013). Unlike fixed-tilt systems, single-axis tracking PVs project non-persistent shadow onto the ground as they constantly rotate to follow the sun's trajectory throughout the day, leading to more complex plant eco-physiological responses that may influence growth, survival, and competitive interactions (Li et al., 2025; Suuronen et al., 2017; Vaverková et al., 2022; Yue et al., 2021). Studies on a single-axis GPV in Colorado, USA, revealed that a cool-season bromegrass shaded in the afternoon exhibited higher g_{sw} and leaf water potential than those shaded in the morning, resulting in a 15% increase in net aboveground productivity (Knapp & Sturchio, 2024; Sturchio et al., 2022; Sturchio et al., 2024).

To date, no eco-physiological studies at GPVs have specifically focused on wildflowers, despite their capstone role in ecological restoration. Ecological restoration is defined as the process of assisting the recovery of a degraded, damaged, or destroyed ecosystem to

reflect values regarded as inherent in the ecosystem and provide ecosystem services that people value (Martin, 2017). Wildflowers support all four types of ecosystem services despite their short height, suggesting a potentially consummate role in ecological restoration at ecovoltaic solar parks where contact between tall plants and GPV infrastructure poses risks (Blaydes et al., 2022, 2024; Dolezal et al., 2021; Graham et al., 2021; Walston et al., 2018, 2023). While the monitoring process can be time-consuming and field-intensive, advances in technology like spectroscopy now allow for non-destructive estimates, reducing the need for prolonged sampling (Serbin et al., 2015). Here, we combined rapid, minimally invasive field techniques with basic laboratory analyses to assess how two perennial wildflowers native to California's Central Valley, with distinct shade and stress tolerances, respond physiologically and morphologically at the leaf level to the microclimatic conditions of a single-axis, tracking GPV.

We hypothesized that, within the array footprint, leaves exposed to greater shadow from PVs would not only experience increased photochemical performance, light-use efficiency, maximum quantum yield, stomatal conductance, transpiratory cooling, and water content, but also develop larger surface areas and chlorophyll pools to compensate for reduced light availability, while accumulating fewer photoprotective pigments, such as carotenoids, anthocyanins, and flavanols (Table 1). We further expected these acclimations to interact with temporal dynamics at both diurnal and seasonal scales, conferring advantages to shade-tolerant species in the afternoon and summertime. Together, our study examines wildflower responses across spatial gradients within the array, temporal variation at both diurnal and

TABLE 1 Abbreviations, descriptions, and predicted responses to shade from single-axis, tracking large, ground-mounted photovoltaic panels for 21 morphological and physiological parameters examined in this study.

No.	Parameter	Abb.	Description	Predicted response to PV shade
1	Specific leaf area	SLA	Leaf area per unit dry mass, indicating resource allocation strategies	Increase due to enhanced needs for light capture
2	Length-to-width ratio	L:W	Leaf shape measure, affecting boundary layer resistance	Increase due to enhanced needs for light capture
3	Maximum quantum yield	Fv/Fm	Potential efficiency of photosystem II in dark-adapted leaves	Increase due to reduced photodamage or photoinhibition
4	Photochemical efficiency	ΦPSII	Proportion of absorbed photons for photochemistry in illuminated leaves	Increase due to lower photoprotective energy dissipation
5	Stomatal conductance	g_{sw}	Rate of gas exchange through stomata, affecting energy-water balance	Increase to maximize CO2 uptake and transpiration
6	Transpiration rate	E	Rate of water loss from leaves via stomata	Decrease due to reduced evaporative cooling demand
7	Leaf vapor pressure deficit	VPD_{leaf}	Driving force for transpiration	Decrease due to greater relative humidity in atmosphere
8	Adjusted leaf temperature	T_{leaf} - AT	Deviation of leaf temperature from ambient air temperature	Decrease due to reduced radiation absorption
9	Crop water stress index	CWSI	Plant water stress based on stomatal closure and transpiration rates	Decrease due to reduced evaporative cooling demand
10	Stomatal conductance index	Ig	Proxy for stomatal function and water use efficiency	Increase due to larger stomatal opening for gas exchange
11	Water band index	WBI	Relative leaf water content based on near-infrared reflectance	Increase due to better water retention
12	Normalized difference Vege index	NDVI	Leaf greenness and overall vegetation health	Increase due to sustained chlorophyll content
13	Photochemical reflectance index	PRI	Xanthophyll cycle activity and light-use efficiency	Decrease due to lower photoprotective energy dissipation
14	Plant senescence reflectance index	PSRI	Leaf senescence and pigment degradation	Decrease due to delayed senescence
15	Carotenoid reflectance index	CRI	Concentration of carotenoids protecting against oxidative stress	Decrease due to reduced need for photoprotection
16	Anthocyanin reflectance index	ARI	Concentration of anthocyanins protecting against UV stress	Decrease due to reduced need for photoprotection
17	Flavanol reflectance index	FRI	Concentration of flavanols protecting against oxidative and UV stress	Decrease due to reduced need for photoprotection
18	Chlorophyll content index	CCI	Total chlorophyll concentration, influencing photosynthetic capacity	Increase due to enhanced needs for light capture

seasonal scales, and species-level differences between the two native perennials, providing a multi-dimensional perspective on plant–PV interactions. These findings offer valuable insights into the plasticity of wildflowers to PV tracking systems, guiding species selection to enhance both ecological and functional co-benefits of restoration efforts in renewable energy landscapes (Hernandez et al., 2019; Sturchio et al., 2024).

2 | METHODS

2.1 | Site description

The experiment was conducted at a 13 MW_{ac} (16.3 MW_{dc}) GPV located in an agricultural landscape near the University of California, Davis (USA; 38.520268, −121.739191). The Central Valley of California is characterized by the Mediterranean climate with annual global horizontal irradiance of 1,854 kWh/m^2, mean temperature of 16.4°C, and annual precipitation of 498 mm (U.S. Climate Data, 2024). Average reference evapotranspiration in Davis was 40 mm, 139 mm, 203 mm, and 101 mm in winter, spring, summer, and autumn, respectively (CIMIS, 2024). The 62-acre (0.251 km^2) single-axis, tracking GPV was constructed in 2015 on a former cropland with Yolo-series soil composed of well-drained loam (SoilWeb, 2024). The multi-crystalline solar modules are mounted on east–west rotating racks, positioned 1.37 m above ground with a pole-to-pole distance of 4.5 m. The site was dominated by nonnative, invasive plants due to the absence of effective weed control measures beyond regular mowing, including but not limited to *Malva neglecta*, *Erodium cicutarium*, and *Festuca perennis* (for more details, see Li et al., 2025).

To explore relationships among tracking GPVs, native prairie establishment, and ecological outcomes, we created eight experimental plots within the array footprint in December 2021, each measuring 23 m in length by 3 m in width. The locations were all carefully selected on level terrain with minimal slope (< 0.3%) and water pooling, and were prepared and sown with a seed mix comprising 11 indigenous wildflower species. The restoration plots were categorized into one of three microenvironments, or micro-patches, based on temporal shading patterns:

a. Two plots shaded in the morning (MS)—areas along the edge of array footprint, bordered by panel strings to the east, receiving direct sunlight during the midday and afternoon (Figure 1c);
b. Two plots shaded in the afternoon (AS)—areas along the edge of array footprint, bordered by panel strings to the west, receiving direct sunlight during the morning and midday (Figure 1d);
c. Four plots shaded in both morning and afternoon (BS)—areas within the array footprint, bordered by panel strings to both the east and west, receiving direct sunlight the during midday only (Figure 1e).

At the time of the restoration, operational constraints and safety regulations precluded restoration activities within areas both without infrastructure installations and directly beneath PV panels—full-sun and full-shade conditions, respectively. Compared with areas without PV installations onsite, MS, AS, and BS experienced 90.9%, 88.0%, and 82.8% of photosynthetic active radiation (PAR), 102%, 89.2%, and 97.8% of vapor pressure deficit (VPD), 77.1%, 70.1%, and 69.4% of wind speed, and 106%, 111%, and 117% of soil moisture, respectively (Li et al., 2025). Post seeding, all plots were managed via hand weeding of non-native exotic plants in early 2022 and 2023.

2.2 | Survey protocol

G. camporum and *P. californica* were selected, as both species: (i) thrived on all plots following a year of establishment (December 2021 – November 2022); (ii) remained viable year-round as perennials, allowing for the assessment of seasonal patterns; (iii) exhibited distinct lifeforms, with *G. camporum* being erect and up to 1.97 m height and *P. californica* growing as a basal rosette up to 1.07 m only; and, (iv) represented contrasting light preferences, with *G. camporum* being sun-loving (Plants For A Future, 2025; Putah Creek Council, 2025) and *P. californica* being shade-tolerant (Gardenia, 2025; Grassroots Ecology, 2022), enabling comparative analysis of plants' responses to the microclimate mosaics introduced by single-axis, tracking GPVs.

A total of 12 surveys were conducted around mid-month from December 2022 to November 2023. At the beginning of each survey, a fully expanded topmost leaf from 15 stems of both wildflower species per micro-patch type was randomly selected (1 leaf × 15 stems × 2 species × 3 micro-patches = 90 leaves) and tagged with a slim, numbered vinyl thread loosely tied to the petiole. Measurements were taken across three time windows—morning (8:30 am – 10:30 am), midday (11:00 am – 1:00 pm), and afternoon (1:30 pm – 3:30 pm)—to (i) capture critical periods of daily microclimate fluctuations and ecophysiological contrasts, and (ii) align with well-accepted methodologies in plant physiological research (Buckley, 2017; Sperry & Love, 2015).

Three calibrated handheld scientific instruments were applied consecutively to the same predefined spot, specifically the central-left portion of the lamina by visually aligning the focus area of each instrument along the midrib and positioned between the primary vein and an adjacent secondary venation, of each marked leaf across all three rounds of sampling per campaign to maintain consistency, following standard protocols:

a. Leaf temperature (T_{leaf}) was recorded by E6 (Teledyne FLIR, Wilsonville, OR, USA; Figure 1h), an infrared imaging camera. To simulate water-limited (T_{dry}) and well-watered (T_{wet}) states, temperatures were also recorded from six additional topmost, fully expanded leaves per micro-patch—three coated with a thin layer of Vaseline and three sprayed with pure water on the adaxial and abaxial surfaces. All measurements were taken at a fixed emissivity of 0.97, with distances kept at 0.2 m and angles avoiding glare effects. Leaves with potential deviations in emissivity were excluded from analysis.

FIGURE 1 Legend on next page.

FIGURE 1 Aerial map of UC Davis Experimental Ecovoltaic Park (a), including plot locations within experimental research area and micro-patches (b), photos of three micro-patches captured at 9:00 am in May 2023: AM shade (; c), PM shade (; d), and AM & PM shade (;e), photos of LI-600 (combined fluorometer and porometer; f), CI-710 s (leaf spectrometer; g), and E6 (thermal IR camera; h) in use on the field, and photos of *Phacelia californica* (i) and *Grindelia camporum* (j) with their leaves scanned and processed by ImageJ. Aerial images (a, b): Google earth; photos c–i: Yudi Li.

b. Φ_{PSII} (unitless), g_{sw} (mol m^{-2} s^{-1}), transpiration (mol m^{-2} s^{-1}; E), leaf VPD (kPa; VPD_{leaf}), PAR (μmol/m^2 s), air temperature (°C; AT), and relative humidity (%; RH) were concurrently recorded by LI-600 (LI-COR, Lincoln, NE, USA; Figure 1f), a combined fluorometer (saturating pulses of ~10,000 μmol/m^2s) and porometer (see Notes S1 & S2 for equations used, respectively). Maximum (F_m) and minimum (F_o) fluorescence of dark-adapted leaves were also recorded at both pre-dawn (4:30 am – 5:30 am) and daytime (10:30 am – 11:00 am or 1:00 pm – 1:30 pm; after foil covering for 45 min).
c. NDVI, PRI, water band index (WBI), plant senescence reflectance index (PSRI), as well as six pigment proxies—carotenoid reflectance index (CRI), anthocyanin reflectance index (ARI), flavanol reflectance index (FRI), chlorophyll content index (CCI), chlorophyll a index, and chlorophyll b index—were automatically derived from reflectance or absorbance (for CCI, chlorophyll a, and chlorophyll b only) spectrums (340 nm – 1,100 nm) recorded by CI-710 s (CID Bio-Science, Portland, WA, USA; Figure 1g), a leaf spectrometer (see Note S3 for equations used by CI-710 s).

At the end of campaigns, all the 90 leaves were harvested, stored in a freezer, and transported to a laboratory at UC Davis where the following parameters were assessed: (i) leaf area (cm^2), maximum length (cm), and maximum width (cm) using a conventional scanner and ImageJ software (Figure 1i–j) (Schneider et al., 2012); and, (ii) biomass (g) after drying the leaves in an oven at 64°C for 72 h.

We further calculated:

1. Vapor pressure deficit (kPa; VPD) based on AT and RH, following Ward and Trimble (2003):

$$VPD = 0.6108 * e^{17.27 * \frac{AT}{AT+273.4}} * \left(1 - \frac{RH}{100}\right)$$

2. Maximum quantum yield (unitless; F_v/F_m) based on pre-dawn dark-adapted F_m and F_o, following Blankenship (2021):

$$F_v/F_m = \frac{F_m - F_o}{F_m}$$

3. Crop water stress index (unitless; CWSI) and stomatal conductance index (Ig; unitless) based on T_{leaf}, T_{dry}, and T_{wet}, following Jones (1999):

$$CWSI = \frac{T_{leaf} - T_{wet}}{T_{dry} - T_{wet}}$$

$$I_g = \frac{T_{dry} - T_{leaf}}{T_{leaf} - T_{wet}}$$

4. Specific leaf area (cm^2/g; SLA) from leaf area and dry biomass, and shape ratio (L/W) from maximum length and width:

$$SLA = \frac{leaf\ area}{dry\ biomass}$$

$$L/W = \frac{maximum\ length}{maximum\ width}$$

2.3 | Data analysis

All statistics were implemented in R 4.2.1 software (R Core Team, Vienna, Austria) using a suite of packages tailored to our diverse datasets. Generalized linear models (GLMs) were fitted to the four meteorological indices (AT, RH, VPD, PAR) and 21 physiological and morphological indices (Table 1) as response variables against species (two levels: *G. camporum* and *P. californica*), micro-patches (three levels: AS, BS, and PS), time of day (three levels: morning, midday, and afternoon), season (four levels: winter—December to February, spring—March to May, summer—June to August, autumn—September to November), and their two-way interactions. Additional GLMs were constructed for the same set of indices against each meteorological and water flux (g_{sw}, E, and VPD_{leaf}) variables, with species as a covariate. Combining these two approaches can effectively disentangle the relative contributions of broad ecological conditions (e.g., seasonality) and specific environmental drivers (e.g., PAR and VPD) in shaping the performance of two native perennial wildflowers within a GPV-impacted landscape.

Error distributions were assessed using the "fitdistrplus" package (Delignette-Muller & Dutang, 2015), fitting Gaussian for real numbers (e.g., AT, NDVI), Beta (with "logit" transformation) for numbers between 0 and 1 (e.g., Φ_{PSII} and CWSI), and Gamma (with "log" transformation) for positive numbers (e.g., VPD and g_{sw}). Model assumptions, such as overdispersion and zero inflation, were evaluated with the "DHARMa" package (Hartig & Lohse, 2022). If violations were detected, GLMs were improved through the "glmmTMB" package (Brooks et al., 2023). Feature selection was guided by the lowest Akaike Information Criterion (AIC) to balance model complexity and explanatory power. For pairwise post hoc comparisons, Tukey's honestly significant difference (HSD) test was applied via the "emmeans" package (Lenth & Lenth, 2018), which inherently corrects for multiple comparisons. While our analyses included a large number of response variables, Tukey HSD effectively controls the Type I error rate, reducing the likelihood of false positives and ensuring that significant differences are statistically robust.

All R scripts used for data analysis and simulation are provided in Code S1, and all raw datasets supporting the results are provided in Dataset S1.

3 | RESULTS

Throughout the day, the leaves of both wildflower species showed a progressive decline in ΦPSII, accompanied by increased transpiration rate, CWSI, and anthocyanin proxy across all micro-patches (Figure 3). No significant differences were observed for g_{sw} and other spectral indices (Figures 3d,f,m,o and S1). CWSI on morning-shade plots ranged from 68% to 96% in the morning and midday but converged with the other two micro-patches in the afternoon during which the differences became no longer significant—mirroring VPD and VPD_{leaf}—while Ig displayed the opposite pattern (Figure 2; Tables S1 and S2). Variations in g_{sw} aligned more strongly with adjusted leaf temperature (inversely) than with transpiration and remained the lowest on morning-shade plots for *P. californica* and midday-sun plots for *G. camporum* until the afternoon (Figures 3d,e,m,n and S1c, l). Both species exhibited the highest WBI and the lowest PSRI and reflectance-based anthocyanin and flavanol indicators on midday-sun plots (Figures 3f,i,l,o,q,r and S1i,t).

Throughout the year: (i) SLA and spectrum proxies of chlorophylls and carotenoids peaked in spring; (ii) maximum quantum yield stabilized from spring onwards (*C. phacelia*: 0.813 ± 0.026; *G. camporum*: 0.820 ± 0.017); (iii) Ig closely tracked VPD, peaking in summer, while CWSI and anthocyanin reflectance index revealed the opposite trends; and, (iv) NDVI and PRI were 1.1 and 10 times higher, respectively, in spring and summer compared with winter and autumn (Figures 2, 4, and S2; Table S3). Differences in SLA and PRI across micro-patches became nonsignificant in summer (Figures 4a,e,l,p and S2a–c,l–n). The length-to-width ratio of *C. phacelia* and *G. camporum* steadily increased and decreased over time, respectively (Figure 4b,n). In summer, transpiration and gsw of *G. camporum* remained comparable to spring levels, with the lowest values observed on midday-sun plots before summer (Figure S2o–p). Conversely, for *P. californica*, they declined by 30% and 24%, respectively, in summer, with the highest values occurring on midday-sun plots (Figure S2d,e; Table S3).

C. phacelia exhibited significantly higher SLA, g_{sw}, Ig, transpiration rate, reflectance-based spectral indices, and most pigment proxies, while lower length-to-width ratio, maximum quantum yield, adjusted leaf temperature, CWSI, and anthocyanin proxy than *G. camporum* across micro-patches($p < 0.05$) (Figures 5 and S3). SLA of *G. camporum* and *C. phacelia* on midday-sun plots was 7%–10% and 13%–20% greater, respectively, than the other two micro-patches (Table S4). Similarly, WBI was the highest on midday-sun plots for both species, followed by afternoon-shade plots, whereas PSRI and spectrum-derived anthocyanin and flavanol levels showcased the opposite trends (Figure 5j,i,n–o). The lowest values of (i) photochemical-related indicators (Φ_{PSII}, PRI) were observed on afternoon-shade plots, and (ii) CWSI and VPD_{leaf} on morning-shade plots (Figures 5d,g,h,l and S3b,c,f). Trends of transpiration and g_{sw} differed between the two species and inversely mirrored adjusted leaf temperature: they peaked on midday-sun plots for *C. phacelia*, whereas *G. camporum* displayed the opposite (Figures 5e,f and S3a).

There was a strong negative correlation between Φ_{PSII} and PAR (adjusted $R^2 = 0.68–0.69$; $p < 0.0001$), with similar coefficients and intercepts between two wildflowers (Figure 6a). Transpiration rate had a moderate positive correlation with both PAR and VPD (adjusted $R^2 = 0.35–0.47$; $p < 0.0001$), with *C. phacelia* consistently showing larger intercepts than *G. camporum* (Figure 6c,j; Table S5). In contrast, adjusted leaf temperature and Ig declined with increasing PAR for both species (adjusted $R^2 = 0.27–0.35$; $p < 0.0001$) (Figure 6g). CWSI and g_{sw} exhibited weak or nonsignificant correlations with all microclimatic variables (Figures 6b,e,i,l and S4b,e,i,l). Both transpiration and adjusted leaf temperature were tightly linked to g_{sw} (positively and negatively, respectively) and inversely correlated with each other (adjusted $R^2 = -0.65 – -0.74$; $p < 0.0001$) (Figure S5j,l,p,q).

4 | DISCUSSION

In this study, we found that micro-patch variation at this single-axis tracking GPV shaped diurnal and seasonal patterns of leaf physiology and morphology in two native wildflowers, despite the results encompassing a single year of measurements from partial-shade conditions within the array footprint. Specifically, our 12-month dataset collected provides valuable insights into the acclimation of native wildflowers, results which inform decision making on species selection for revegetation efforts and, thus, the transition toward ecovoltaics. Further, our results may be useful considering that (i) many perennials function as facultative biennials or even annuals in arid and semi-arid regions like the Central Valley of California (Amos et al., 2024); (ii) the three micro-patches we studied collectively account for a substantial share of the total GPV area (e.g., 47% in our case; Li et al., 2025); and (iii) the 18 indices we measured are well-established indicators of plant performance and stress.

The microclimatic heterogeneity imposed spatially across the three micro-patches was insufficient to alter leaf shape, maximum quantum yield, greenness (NDVI), or spectrally derived carotenoid and chlorophyll levels in both species (Figures 5 & S3) (Lim & Kim, 2021). More pronounced changes in chlorophyll content, as reported in studies such as Dai et al. (2009) and Semeraro et al. (2024), may occur under higher interception of incident radiation (e.g., >25%), such as the micro-patch directly beneath PV modules. However, stems growing in midday-sun plots, subjected to 7%–9% more shade and shorter photoperiods, exhibited notable morphological and physiological adjustments of leaves, including: (i) 7%–20% larger specific leaf area (SLA), indicating expanded area to promote light capture at the expense of thickness; (ii) 14%–27% and 8%–18% reductions in the proxies of anthocyanin and flavanol, respectively, suggesting decreased photoprotection; (iii) up to 200% decrease in Plant Senescence Reflectance Index (PSRI), signaling healthier conditions, such as delayed senescence; and, (iv) 1.2%–1.6% higher Water Band Index (WBI), reflecting enhanced water retention that is critical in drought-

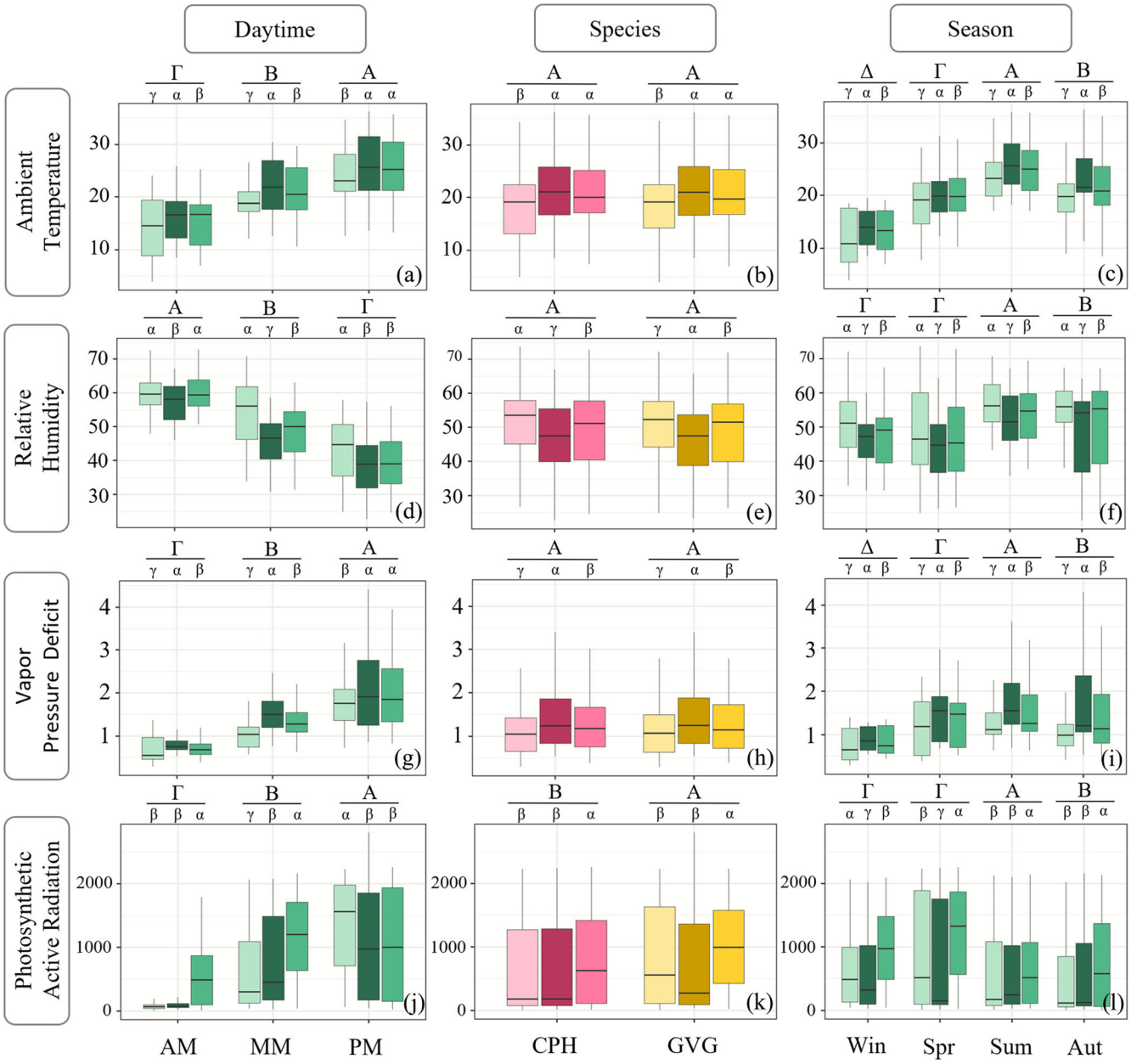

FIGURE 2 Boxplots of ambient temperature (°C; a–c), relative humidity (%;d–f), vapor pressure deficit (kPa; g–i), and photosynthetic active radiation (μmol m^{-2} s^{-1}; j–l) across three micro-patches – MS (morning-shade; lighter color), BS (midday-sun; darker color), AS (afternoon-shade; normal color) – faceted by four seasons (win – winter, Spr – spring, sum – summer, Aut – autumn), three daytimes (AM – morning, MM – midday, PM – afternoon), and two species (CPH – *Phacelia californica*, GVG – *Grindelia camporum*) at the UC Davis experimental Ecovoltaic Park (Davis, California, United States). Statistical differences between levels, as determined by Tukey's honestly significant difference (HSD) test, are denoted using Greek symbols (e.g., α, β, γ).

prevailing semiarid regions (Figure 5a,m-o; Table S4) (Fagnano et al., 2024; Jagodziński et al., 2016; Lambert et al., 2022). Although the vapor pressure deficit of midday-sun plots was 1.2 times that of the other two micro-patches, the elevated transpiration demand may be offset by a combined 11% greater soil moisture and 8% slower wind speed, as we reported in Li et al. (2025) at the same GPV (Table 2.h), contributing to a thicker boundary layer resistance under attenuated direct airflow. Significantly higher WBI of both species on afternoon-shade than morning-shade plots also highlighted the benefits of shade to maintain water balance in leaves (Figure 5j) (Barron-Gafford et al., 2019; Kannenberg et al., 2023; Sturchio & Knapp, 2023).

Diurnally, physiological parameters of instantaneous responses were influenced by a combination of meteorological conditions and PV panel rotation, as hypothesized. Photosynthetically active radiation was a primary driver of chlorophyll fluorescence, with photochemical efficiency (Φ_{PSII}) in both perennials progressively declining from 8:30 a.m. to 3:30 p.m. (Figures 3a,l and 6a–c,j–l) due to

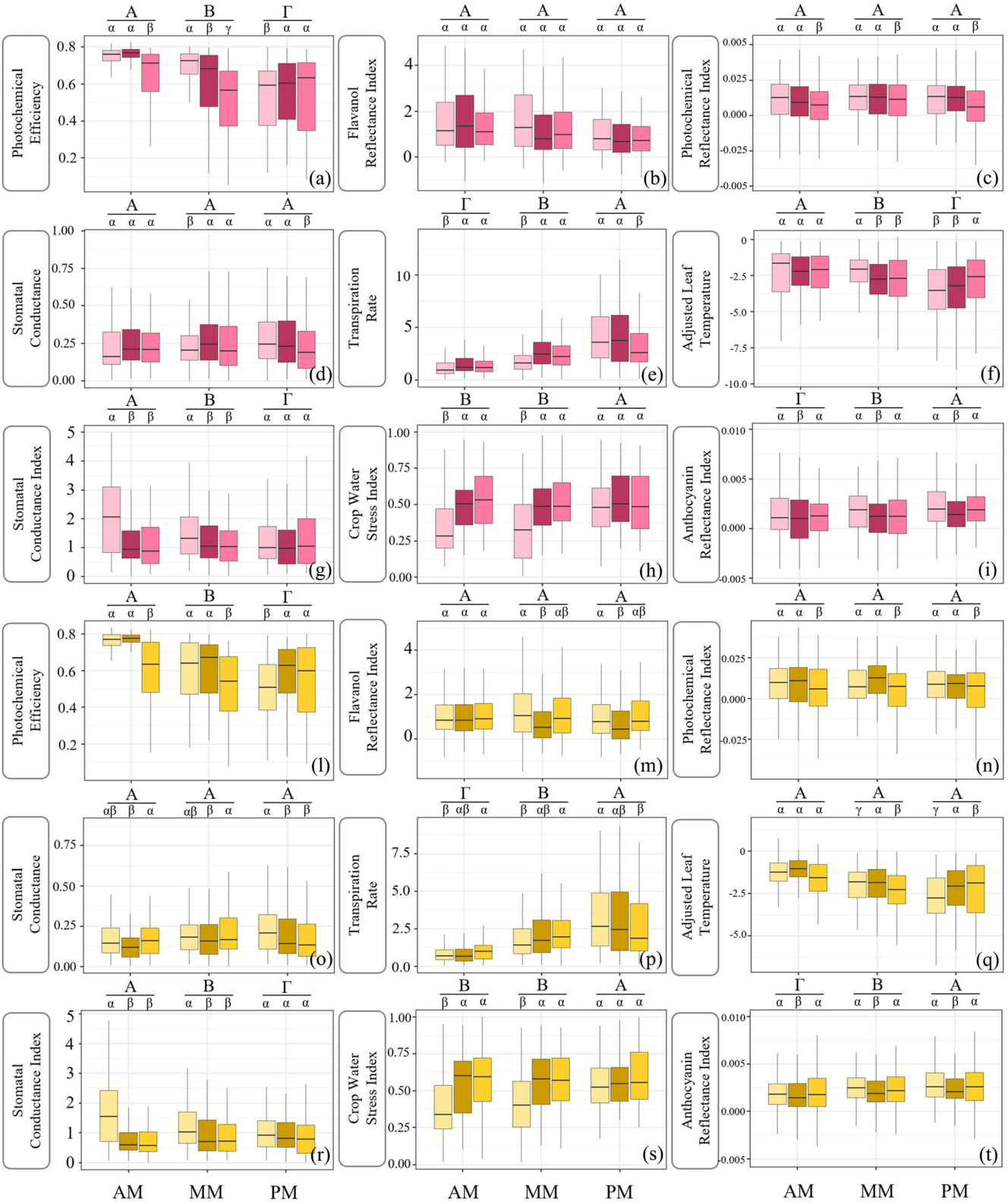

FIGURE 3 Boxplots of photochemical efficiency (Φ_{PSII}; unitless), flavanol reflectance index (FRI; unitless), photochemical reflectance index (PRI; unitless), stomatal conductance (g_{sw}; Mol m^{-2} s^{-1}), transpiration rate (E; Mol m^{-2} s^{-1}), water band index (WBI; unitless), stomatal conductance index (Ig; unitless), crop water stress index (CWSI; unitless), and anthocyanin reflectance index (ARI; unitless) across three micro-patches – MS (morning-shade; lighter color), BS (midday-sun; darker color), AS (afternoon-shade; normal color) – over three daytimes (AM – morning, MM – midday, PM – afternoon) for *Phacelia californica* (a–i) and *Grindelia camporum* (l–t) at the UC Davis experimental Ecovoltaic Park (Davis, California, United States). Statistical differences between levels, as determined by Tukey's honestly significant difference (HSD) test, are denoted using Greek symbols (e.g., α, β, γ).

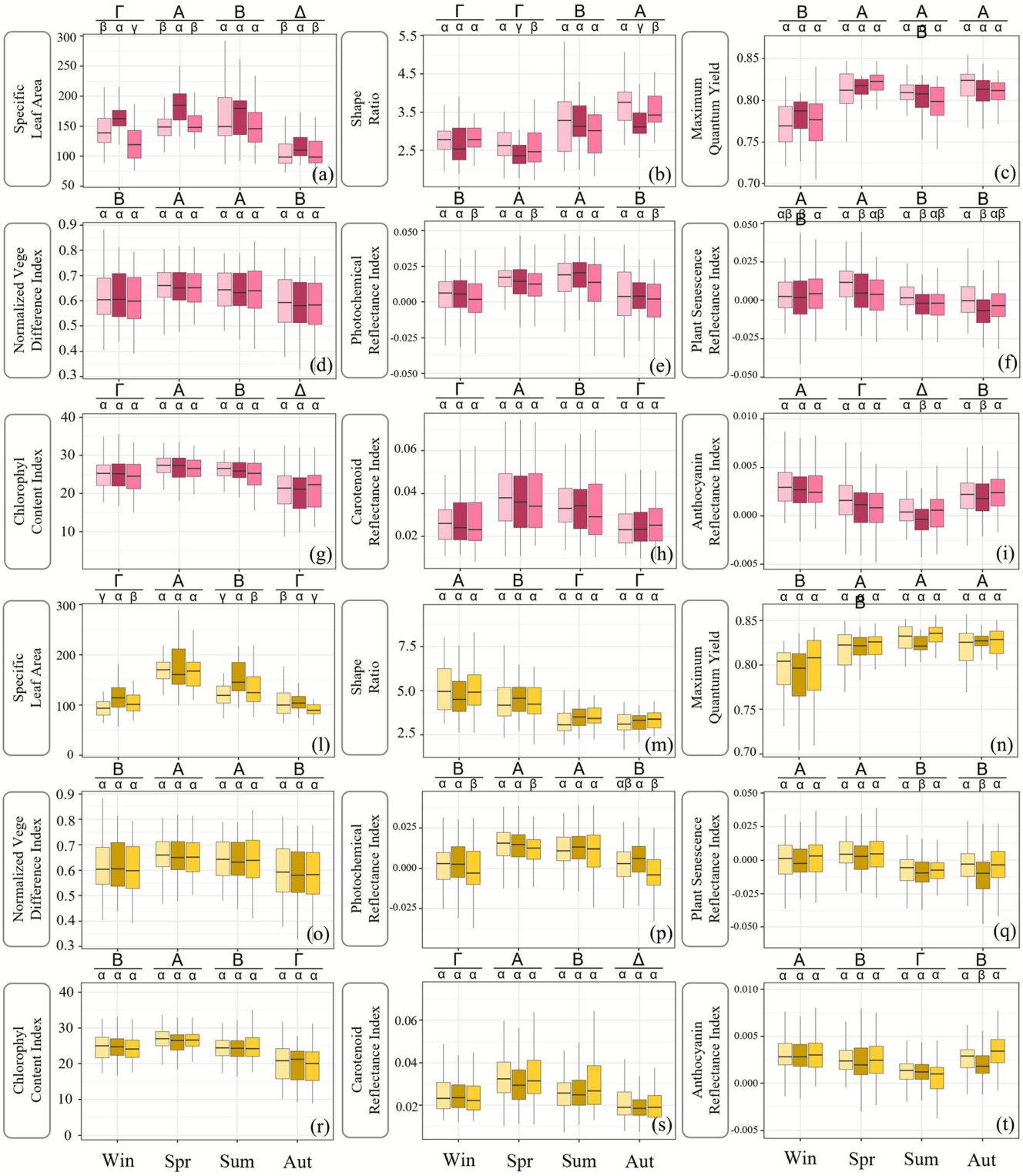

FIGURE 4 Boxplots of specific leaf area (SLA; unitless), length-to-width ratio (L/W; unitless), maximum quantum yield (F_v/F_m; unitless), normalized difference vegetation index (NDVI; unitless), photochemical reflectance index (PRI: unitless), plant senescence reflectance index (PSRI; unitless), chlorophyll content index (CCI; unitless), carotenoid reflectance index (CRI; unitless), and anthocyanin reflectance index (ARI; unitless) across three micro-patches – MS (morning-shade; lighter color), BS (midday-sun; darker color), AS (afternoon-shade; normal color) – over four seasons (win – winter, Spr – spring, sum – summer, Aut – autumn) for *Phacelia californica* (a–i) and *Grindelia camporum* (l–t) at the UC Davis experimental Ecovoltaic Park (Davis, California, United States). Statistical differences between levels, as determined by Tukey's honestly significant difference (HSD) test, are denoted using Greek symbols (e.g., α, β, γ).

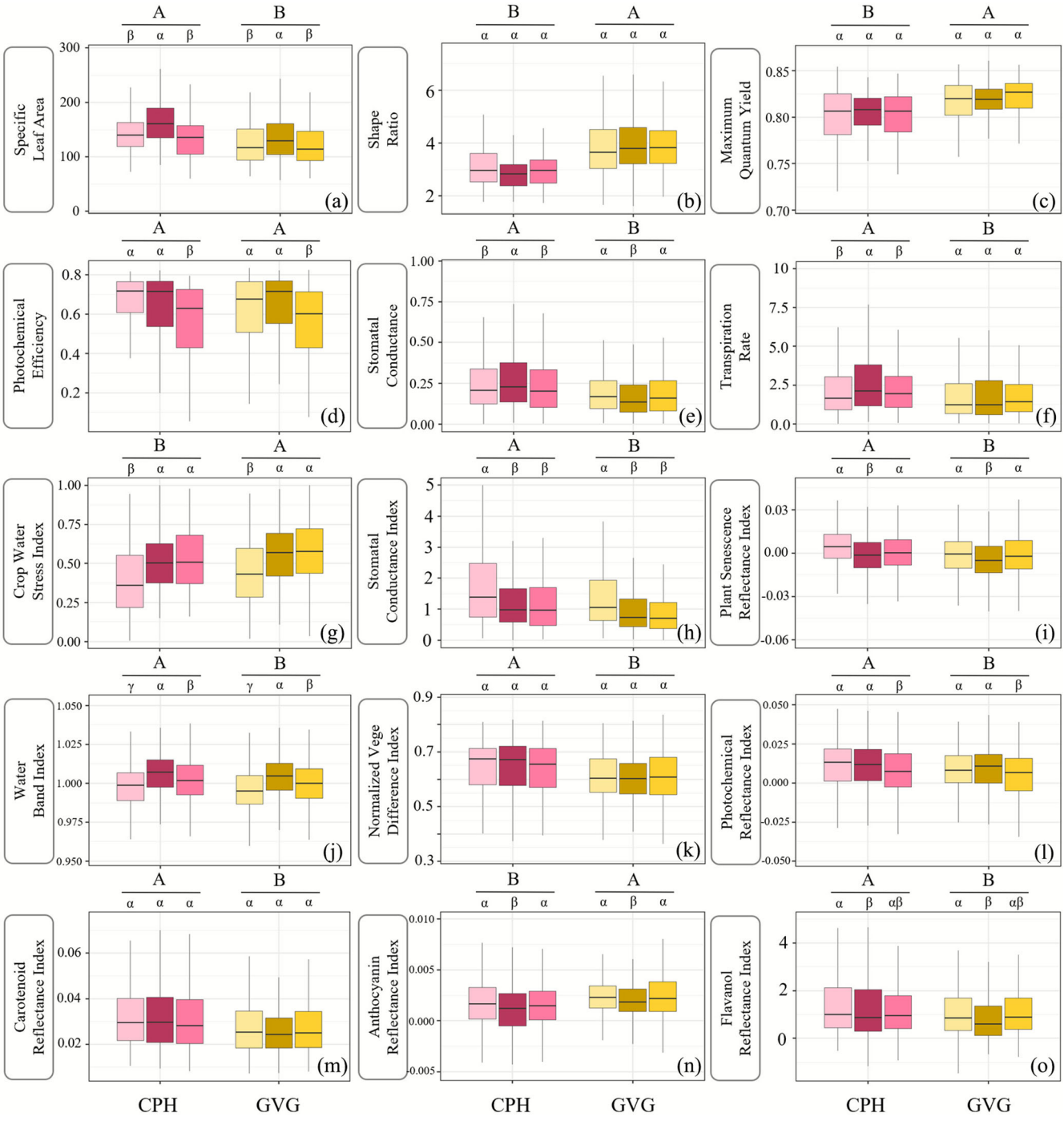

FIGURE 5 Boxplots of specific leaf area (SLA; unitless; a), length-to-width ratio (L/W; unitless; b), maximum quantum yield (F_v/F_m; unitless; c), photochemical efficiency (Φ_{PSII}; unitless; d), stomata conductance (g_{sw}; Mol m^{-2} s^{-1}; e), transpiration rate (E; Mol m^{-2} s^{-1}; f), crop water stress index (CWSI; unitless; g), stomata conductance index (Ig; unitless; h), plant senescence reflectance index (PSRI; unitless; i), water band index (WBI; unitless; j), normalized difference vegetation index (NDVI; unitless; k), photochemical reflectance index (PRI: unitless; l), carotenoid reflectance index (CRI, unitless; m), anthocyanin reflectance index (ARI; unitless; n), and flavanol reflectance index (FRI; unitless; o) across three micro-patches – MS (morning-shade; lighter color), BS (midday-sun; darker color), AS (afternoon-shade; normal color) – between two species (CPH – *Phacelia californica*, GVG – *Grindelia camporum*) at the UC Davis experimental Ecovoltaic Park (Davis, California, United States). Statistical differences between levels, as determined by Tukey's honestly significant difference (HSD) test, are denoted using Greek symbols (e.g., α, β, and γ).

photosynthetic compromised capacity to harvest photons (Figure 2j) (Cuzzuol et al., 2020; Franck & Vaast, 2009; Grassi et al., 2009; Narayanan et al., 2015). This was coincident with the escalation of (i) anthocyanin proxy, consistent with previous findings on photoprotective pigment accumulation under light stress, which may also be driven by changes in pH, water potential, or antioxidant reaction

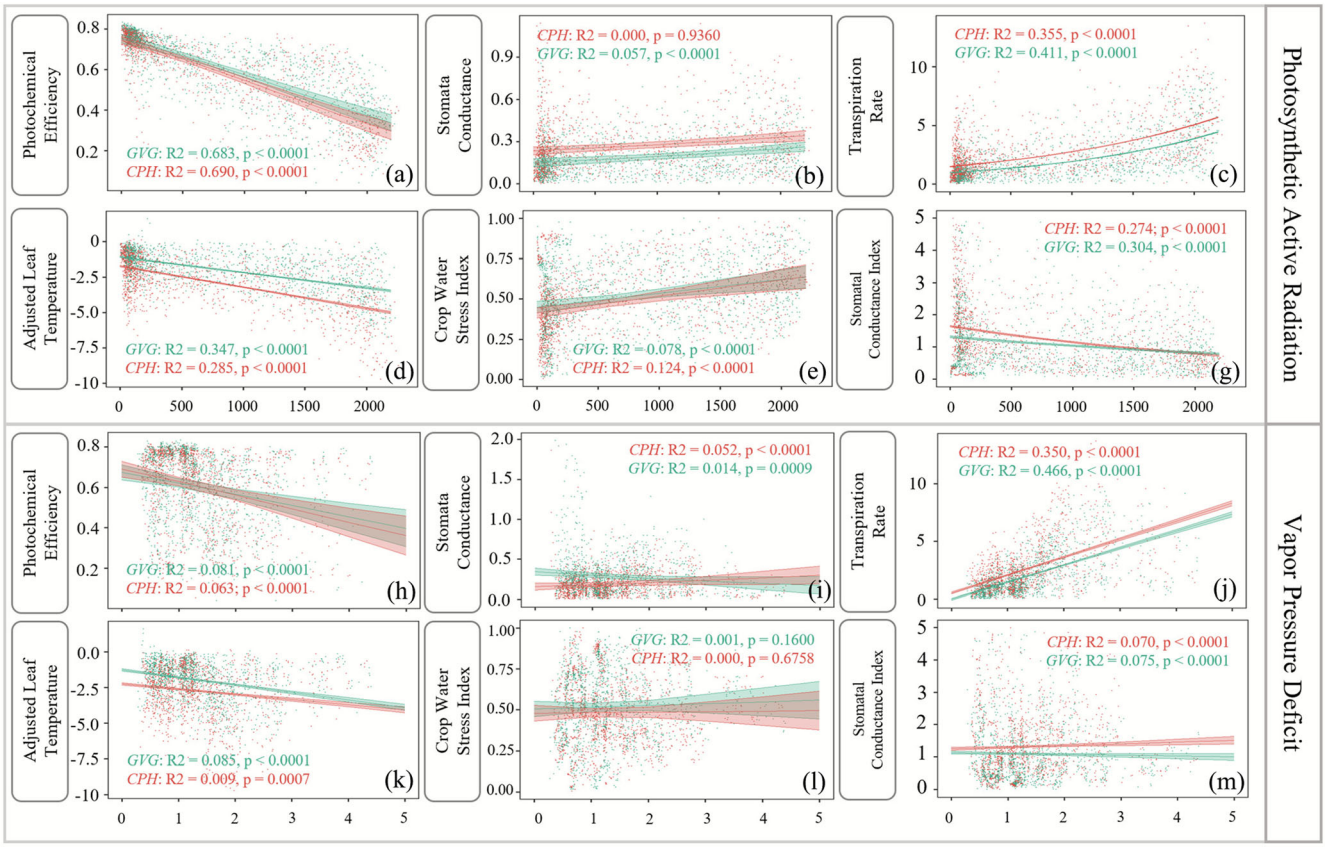

FIGURE 6 Best-fitted GLM models of photochemical efficiency (ΦPSII; unitless), photochemical quenching (qP; unitless), non-photochemical quenching (NPQ; unitless), stomata conductance (g_{sw}; Mol m^{-2} s^{-1}), transpiration rate (E; Mol m^{-2} s^{-1}), adjusted leaf temperature (T_{leaf} – AT; °C), crop water stress index (CWSI; unitless), stomata conductance index (Ig; unitless; h) against photosynthetic active radiation (PAR, μmol m^{-2} s^{-1}; a–i) and vapor pressure deficit (VPD, kPa; j–r) for *Phacelia californica* (CPH; red) and *Grindelia camporum* (GVG; green) at the UC Davis experimental Ecovoltaic Park (Davis, California, United States). Adjusted R^2 and *p*-values are labeled at species level.

(Figure 3i,t) (Hatier & Gould, 2009; Hughes, 2011); and, (ii) transpiration rate, indicating reliance on evaporative cooling to regulate leaf temperature, as reflected by larger differentials with ambient temperature that came at the cost of higher risk of hydraulic failure, evidenced by elevated Crop Water Stress Index (CWSI) and lowered stomatal conductance index (Ig) (Figure 3e–h,p–s) (Grossiord et al., 2020; Rinza et al., 2021). The transient fluctuations in leaf anthocyanin proxies were unlikely to be solely an optical artifact given the absence of transient fluctuations in the other measured pigments (Figure S1e–g,m–o) (Merzlyak et al., 2008). Shadow cast by PV panels in the morning and midday effectively prompted the leaf photochemical (i.e., Φ_{PSII} and PRI) and hydro-thermal (i.e., transpiration and CWSI) performances on morning-shaded plots, the advantages of which on afternoon-shaded plots diminished in the afternoon when vapor pressure deficit remained high (also observed in Knapp & Sturchio, 2024)—as the heat emission from adjacent operating panels was also the greatest during the day (Figure 3).

Contrary to our hypothesis, seasonal benefits of panel shading were not more pronounced in summer, likely because plant ontogeny exerted a stronger influence at this scale (Figures 2, 4, and S2) (Mänd et al., 2010; Poorter et al., 2019). This was particularly prominent in the divergent trends of leaf length-to-width ratio between the two perennials: *G. camporum* shifted toward a more drought-resistant shape with reduced elongation from December 2022 to November 2023, while *P. californica* developed increasingly longer, narrower leaves to enhance heat dissipation and optimize photosynthesis over time (Figure 4b,m) (Poorter et al., 2009; Valladares & Niinemets, 2008). SLA and spectrally derived indicators of carotenoid and chlorophyll content in both species peaked in spring coinciding with active growth by prioritizing resource acquisition via leaf area enlargement and pigment accumulation to maximize light harvesting while preemptively reinforcing photoprotective mechanisms in anticipation of oxidative stress in summer (Figure 4a,g,h,l,r,s) (Jagodziński et al., 2016; Lambers et al., 2008; Niinemets, 2010; Pompodakis et al., 2005). The relatively stable maximum quantum yield, above 0.80, spring through autumn across all three micro-patches demonstrated their capacities in sustaining photochemical functions (Figure 4c,n) (Colom & Vazzana, 2003; Lichtenthaler et al., 2007). Significant decreases of NDVI (−8%) and PRI (−92%) from summer to autumn signaled a transition out of peak growth (Figure 4d, o, p; Table S3) (Gamon et al., 2015). The reduced incident radiation measured during summer compared with spring caused by denser

vegetation canopies and thus interspecific shading, may explain the sharp declines in flavanol proxies and PSRI, particularly in *C. phacelia* which has a low-stature rosette form (Figures 2l, 4f,q, and S2c,k,n,v) (Behmann et al., 2014; Tölgyesi et al., 2023).

While both native wildflowers thrived within the array footprint, *P. californica* was proven to be particularly well-suited for environments with partial shades, evident through an ensemble of superior performances, including significantly higher SLA (1.13 times), width-to-length ratio (1.27 times), light-use efficiency (PRI; 1.38 times), transpiration rate (1.32 times), greenness (NDVI; 1.06 times), and pools of chlorophyll (1.03 times) and flavanol (1.45 times) than those in *G. camporum* (Figure 5; Table S4) (de Casas et al., 2011; Wang et al., 2020). Notably, the increase of SLA in *P. californica* on midday-sun plots compared with the other two micro-patches (+14%–20%) was twice that of *G. camporum* (+7%–10%), showcasing a more plastic morphological change in response to induced shade (Wynne-Sison et al., 2023). *P. californica* also maintained greater stomatal conductance (g_{sw}) on midday-sun plots, suggesting the prioritization of carbon gain over water retention through prolonged stomatal opening even under higher vapor pressure deficit; whereas the leathery leaves of *G. camporum* exhibited the opposite pattern, implying a more conservative, isohydric strategy that warrants further investigation through direct measurements of leaf water potential under a gradient of soil moistures (Figures 2h and 5e) (Grossiord et al., 2018; Urban et al., 2017). Despite the large standard errors associated with g_{sw}, it is known to fluctuate dynamically, and even slight variability can have significant ecological implications (Table S4) (Buckley, 2017; Klein, 2014; McDowell et al., 2008; Sperry & Love, 2015). Regardless, *G. camporum* successfully established and proliferated at this site, challenging its classification as strictly sun-loving documented by some authoritative California plant databases (Mahanty, 2023). In our context, *G. camporum* could be instead characterized as a competitor and *P. californica* as a stress-tolerator to better reflect their differing life history strategies and sensitivities to factors beyond sunlight availability (Ferrara et al., 2023).

For future eco-physiological studies of leaves at GPVs, selecting parameters and instruments based on temporal scale could enhance understanding. Fluorometers, porometers, and infrared cameras effectively capture diurnal, instantaneous dynamics, while spectral indices and functional traits provide additional insights into seasonal trends (Gerhards et al., 2016; Pompodakis et al., 2005). Combining multiple techniques can offer complementary perspectives on the intricate mechanisms governing plant energy-water balance (Drake et al., 2013; Aubrecht et al., 2016; Furtak & Nosalewicz, 2022). For example, while we found evidence supporting the constraint of high leaf vapor pressure deficit on stomatal aperture in *G. camporum*, as reported for a perennial bromegrass by Sturchio et al. (2024), this effect was only marginally significant for *P. californica*. Instead, g_{sw} was strongly correlated with adjusted leaf temperature ($R^2 = 0.51$–0.61), highlighting the primary role of stomatal regulation in preventing leaf overheating (Figure S5) (Michaletz et al., 2016; Urban et al., 2017).

However, the decoupling between Ig and g_{sw} and between PRI and Φ_{PSII} underscored the potential biases and necessary cautions when relying solely on a single thermal or spectral instrument to indirectly assess leaf physiological responses without verification from direct, established methodologies (Craparo et al., 2017; Gamon & Berry, 2012; Gamon & Bond, 2013). Another caveat was the use of spectrally derived proxies without calibration against extracted pigments: aside from potential deviations, their mass-based concentrations could not be calculated, which may help explain the absence of significant differences in carotenoid and chlorophyll levels across micro-patches, as well as the counterintuitive seasonal patterns observed in anthocyanin—all were estimated on a per-area basis (Figures 4r–t, 5m, and S3d,e) (Croft et al., 2017; Mahanty, 2023). While these spectroscopic pigment parameters may lack the exact quantitative precision of traditional methods, they offer scalable, non-destructive, and cost-effective insights into the diversity of micro-patches created by GPV infrastructure and its operation to inform ecological restoration management decisions related to plant stress.

A major limitation of this study is that it covers only a single year (December 2022 to November 2023) in the lifecycle of these approximately 1-year-old perennials and, thus, results should not be temporally extrapolated beyond this period, as they often exhibit delayed or cumulative responses—that is, legacy effects – to altered environments driven by annual variations. On the other hand, the absence of full-sun (open spaces) and full-shade (beneath PV panels) controls limits the extent to which we can evaluate the plant acclimation across the full microclimatic gradient (i.e., "micro-patches") typical of GPVs. Consequently, we cannot conclusively determine whether their growth was enhanced or suppressed, as direct extrapolation may be erroneous, and as relationships with light levels can be non-linear and compounded by other abiotic and biotic factors like ambient temperature, soil moisture, and intra- and inter-specific competition.

With our industry and community partners, we have facilitated the re-vegetation of the single-axis, tracking GPV (i.e., across all micro-patches within the array footprint) with diverse, native seed mixtures since late 2024, enabling longer-term, multi-year eco-physiological assessments across a broader range of environmental heterogeneity, management practices (e.g., mowing and grazing), and herbaceous species. Future studies to expand our measurements include: (i) carbon fixation, which does not always correlate linearly with Φ_{PSII} (Baker, 2008; Magney et al., 2020); (ii) pigment and nutrient content (e.g., nitrogen and potassium) through chemical extraction followed by high-pressure liquid chromatography to improve the calibration of spectral indices; (iii) tissue-level assessments beyond leaves, such as net productivity, relative growth rate, biomass allocation, and other functional traits to provide a more comprehensive evaluation of acclimation (Halbritter et al., 2020); and (iv) additional microclimate parameters to refine our scientific grasp of interactions with PV infrastructures (Maes & Steppe, 2012).

5 | CONCLUSION

This study showcases the role of single-axis, tracking GPVs in driving microclimate variation, particularly through changes in radiation exposure and heat loads, and their subsequent effects on the physiological

and morphological traits of native perennial wildflowers. Spatially, even subtle differences in the microclimate conditions—known as micro-patches—within the array footprint resulted in distinct eco-physiological acclimations, with afternoon shading proving particularly beneficial for water conservation in both species (Li et al., 2025). Temporally, we found that diurnal dynamics of leaf physiology were driven by the combined effects of the microclimatic conditions created by PV panels and their rotation, while seasonal trends in leaf physiology were shaped predominantly by plant ontogeny. *P. californica* exhibited traits associated with stress tolerance, such as greater SLA, light-use efficiency, transpiration rate, and pigment accumulation in partially shaded environments, whereas *G. camporum* displayed more conservative traits, thriving in a range of light conditions if the risk of water loss was minimized. Thus, framing them simply as "shade-tolerant" and "sun-loving" may overlook their nuanced adaptive strategies. Therefore, relying on certain online databases—which may miscategorize *G. camporum* or other native species as strictly "sun-loving" or "shade-intolerant"—could lead to their exclusion from seed selection within the array footprint, despite their potential to thrive under such conditions. This, in turn, may result in missed opportunities, ecologically and economically, for solar developers to enhance botanical and structural diversity at their projects. Moving forward, we aim to expand long-term eco-physiological assessments across a broader spectrum of microclimates, species, indicators, and methodologies to not only deepen the understanding of the interplay between vegetation and GPVs, but to also optimize strategic planning for ecovoltaic solar parks.

AUTHOR CONTRIBUTIONS

Yudi Li, Troy Magney, and Rebecca R. Hernandez conceived and designed the experiment. Yudi Li collected and analyzed the data and wrote the manuscript with input from Yudi Li, Troy Magney, Alona Armstrong, and Rebecca R. Hernandez.

ACKNOWLEDGEMENTS

We want to express our gratitude to the Electric Power Research Institute and the University of California Office of the President's California Climate Action Seed Grant (Award A24-1267). Additional funding for RRH and YL was provided by the Agricultural Experiment Station Hatch projects CA-R-A-6689-H and CA-D-LAW-2352-H and the Department of Land, Air, and Water Resources at the University of California, Davis. We also appreciate the long-term coordination from the project owner, Arevon Energy, which provided access and support for the ecological restoration and vegetation monitoring conducted onsite.

CONFLICT OF INTEREST STATEMENT

The authors declare that there is no known conflict of interest.

DATA AVAILABILITY STATEMENT

The data supporting this study's findings are included in the Supporting Information.

ORCID

Yudi Li https://orcid.org/0000-0002-7143-838X
Alona Armstrong https://orcid.org/0000-0001-8963-4621
Rebecca R. Hernandez https://orcid.org/0000-0002-8031-2949

REFERENCES

Amos, C. H., Richardson, B. A., Barga, S., Kilkenny, F. F., & Kasten Dumroese, R. (2024). Annual-perennial lifespan variation in *Chaenactis douglasii* suggests a drought escape strategy in warm-arid environments. *American Journal of Botany*, *111*(9), e16391. https://doi.org/10.1002/ajb2.16391

Armstrong, A., Ostle, N. J., & Whitaker, J. (2016). Solar park microclimate and vegetation management effects on grassland carbon cycling. *Environmental Research Letters*, *11*(7), 074016. https://doi.org/10.1088/1748-9326/11/7/074016

Aubrecht, D. M., Helliker, B. R., Goulden, M. L., Roberts, D. A., Still, C. J., & Richardson, A. D. (2016). Continuous, long-term, high-frequency thermal imaging of vegetation: Uncertainties and recommended best practices. *Agricultural and Forest Meteorology*, *228*, 315–326.

Baker, N. R. (2008). Chlorophyll fluorescence: A probe of photosynthesis in vivo. *Annual Review of Plant Biology*, *59*, 89–113. https://doi.org/10.1146/annurev.arplant.59.032607.092759

Barron-Gafford, G. A., Pavao-Zuckerman, M. A., Minor, R. L., Sutter, L. F., Barnett-Moreno, I., Blackett, D. T., & Macknick, J. E. (2019). Agrivoltaics provide mutual benefits across the food–energy–water nexus in drylands. *Nature Sustainability*, *2*(9), 848–855. https://doi.org/10.1038/s41893-019-0364-5

Behmann, J., Steinrücken, J., & Plümer, L. (2014). Detection of early plant stress responses in hyperspectral images. *ISPRS Journal of Photogrammetry and Remote Sensing*, *93*, 98–111. https://doi.org/10.1016/j.isprsjprs.2014.03.016

Blankenship, R. E. (2021). *Molecular mechanisms of photosynthesis*. John Wiley & Sons.

Blaydes, H., Gardner, E., Whyatt, J. D., Potts, S. G., & Armstrong, A. (2022). Solar park management and design to boost bumble bee populations. *Environmental Research Letters*, *17*(4), 044002. https://doi.org/10.1088/1748-9326/ac5840

Blaydes, H., Potts, S. G., Whyatt, J. D., & Armstrong, A. (2024). On-site floral resources and surrounding landscape characteristics impact pollinator biodiversity at solar parks. *Ecological Solutions and Evidence*, *5*(1), e12307. https://doi.org/10.1002/2688-8319.12307

Brooks, M., Bolker, B., Kristensen, K., Maechler, M., Magnusson, A., & McGillycuddy, M. (2023). Package 'glmmtmb'. R Packag Vers, 1(1), 7.

Buckley, T. N. (2017). Modeling stomatal conductance. *Plant Physiology*, *174*(2), 572–582. https://doi.org/10.1104/pp.16.01772

California Irrigation Management Information System (CIMIS). (2024). Weather and evapotranspiration data for California agriculture. California Department of Water Resources https://cimis.water.ca.gov

Carins Murphy, M. R., Jordan, G. J., & Brodribb, T. J. (2012). Differential leaf expansion can enable hydraulic acclimation to sun and shade. *Plant, Cell & Environment*, *35*(8), 1407–1418. https://doi.org/10.1111/j.1365-3040.2012.02498.x

Colom, M. R., & Vazzana, C. (2003). Photosynthesis and PSII functionality of drought-resistant and drought-sensitive weeping lovegrass plants. *Environmental and Experimental Botany*, *49*(2), 135–144. https://doi.org/10.1016/S0098-8472(02)00065-5

Craparo, A. C. W., Steppe, K., Van Asten, P. J., Läderach, P., Jassogne, L. T., & Grab, S. W. (2017). Application of thermography for monitoring stomatal conductance of *Coffea arabica* under different shading systems. *Science of the Total Environment*, *609*, 755–763. https://doi.org/10.1016/j.scitotenv.2017.07.158

Croft, H., Chen, J. M., Luo, X., Bartlett, P., Chen, B., & Staebler, R. M. (2017). Leaf chlorophyll content as a proxy for leaf photosynthetic

capacity. *Global Change Biology*, *23*(9), 3513–3524. https://doi.org/10.1111/gcb.13599

Cuzzuol, G. R. F., Gama, V. N., Zanetti, L. V., Werner, E. T., & Pezzopane, J. E. M. (2020). UV-B effects on growth, photosynthesis, total antioxidant potential and cell wall components of shade-tolerant and sun-tolerant ecotypes of *Paubrasilia echinata*. *Flora*, *271*, 151679. https://doi.org/10.1016/j.flora.2020.151679

Dai, Y., Shen, Z., Liu, Y., Wang, L., Hannaway, D., & Lu, H. (2009). Effects of shade treatments on the photosynthetic capacity, chlorophyll fluorescence, and chlorophyll content of Tetrastigma hemsleyanum Diels et Gilg. *Environmental and Experimental Botany*, *65*(2–3), 177–182. https://doi.org/10.1016/j.envexpbot.2008.12.008

de Casas, R. R., Vargas, P., Pérez-Corona, E., Manrique, E., García-Verdugo, C., & Balaguer, L. (2011). Sun and shade leaves of Olea europaea respond differently to plant size, light availability and genetic variation. *Functional Ecology*, *25*(4), 802–812. https://doi.org/10.1111/j.1365-2435.2011.01851.x

Delignette-Muller, M. L., & Dutang, C. (2015). Fitdistrplus: An R package for fitting distributions. *Journal of Statistical Software*, *64*, 1–34. https://doi.org/10.18637/jss.v064.i04

Dolezal, A. G., Torres, J., & O'Neal, M. E. (2021). Can solar energy fuel pollinator conservation? *Environmental Entomology*, *50*(4), 757–761. https://doi.org/10.1093/ee/nvab041

Drake, P. L., Froend, R. H., & Franks, P. J. (2013). Smaller, faster stomata: Scaling of stomatal size, rate of response, and stomatal conductance. *Journal of Experimental Botany*, *64*(2), 495–505. https://doi.org/10.1093/jxb/ers347

Dubey, R. S. (2018). Photosynthesis in plants under stressful conditions. In *Handbook of photosynthesis* (pp. 629–649). CRC Press. https://doi.org/10.1201/9781315372136-34

Dupraz, C., Marrou, H., Talbot, G., Dufour, L., Nogier, A., & Ferard, Y. (2011). Combining solar photovoltaic panels and food crops for optimising land use: Towards new agrivoltaic schemes. *Renewable Energy*, *36*(10), 2725–2732. https://doi.org/10.1016/j.renene.2011.03.005

Fagnano, M., Fiorentino, N., Visconti, D., Baldi, G. M., Falce, M., Acutis, M., Genovese, M., & Di Blasi, M. (2024). Effects of a photovoltaic plant on microclimate and crops' growth in a Mediterranean area. *Agronomy*, *14*(3), 466. https://doi.org/10.3390/agronomy14030466

Fernández-Bou, A. S., & Yang, V. (2024). Agrivoltaics and ecovoltaics: How solar power can deliver water savings, farm success, and a healthier environment. Retrieved November 13, 2024, from https://www.ucs.org/sites/default/files/2024-07/Agrivoltaics-and-Ecovoltaics-eng_0.pdf

Ferrara, G., Boselli, M., Palasciano, M., & Mazzeo, A. (2023). Effect of shading determined by photovoltaic panels installed above the vines on the performance of cv. Corvina (Vitis vinifera L.). *Scientia Horticulturae*, *308*, 111595. https://doi.org/10.1016/j.scienta.2022.111595

Franck, N., & Vaast, P. (2009). Limitation of coffee leaf photosynthesis by stomatal conductance and light availability under different shade levels. *Trees*, *23*, 761–769. https://doi.org/10.1007/s00468-009-0318-z

Furtak, A., & Nosalewicz, A. (2022). Leaf-to-air vapor pressure deficit differently affects barley depending on soil water availability. *South African Journal of Botany*, *146*, 497–502. https://doi.org/10.1016/j.sajb.2021.11.043

Gamon, J. A., & Berry, J. A. (2012). Facultative and constitutive pigment effects on the photochemical reflectance index (PRI) in sun and shade conifer needles. *Israel Journal of Plant Sciences*, *60*(1–2), 85–95. https://doi.org/10.1560/IJPS.60.1-2.85

Gamon, J. A., & Bond, B. (2013). Effects of irradiance and photosynthetic downregulation on the photochemical reflectance index in Douglas-fir and ponderosa pine. *Remote Sensing of Environment*, *135*, 141–149. https://doi.org/10.1016/j.rse.2013.03.032

Gamon, J. A., Kovalchuck, O., Wong, C. Y. S., Harris, A., & Garrity, S. R. (2015). Monitoring seasonal and diurnal changes in photosynthetic pigments with automated PRI and NDVI sensors. *Biogeosciences*, *12*(13), 4149–4159. https://doi.org/10.5194/bg-12-4149-2015

Gardenia. (2025). Phacelia californica (California phacelia). Gardenia.net. Retrieved March 7, 2025, from https://www.gardenia.net/plant/phacelia-californica

Gerhards, M., Rock, G., Schlerf, M., & Udelhoven, T. (2016). Water stress detection in potato plants using leaf temperature, emissivity, and reflectance. *International Journal of Applied Earth Observation and Geoinformation*, *53*, 27–39. https://doi.org/10.1016/j.jag.2016.08.004

Graham, M., Ates, S., Melathopoulos, A. P., Moldenke, A. R., DeBano, S. J., Best, L. R., & Higgins, C. W. (2021). Partial shading by solar panels delays bloom, increases floral abundance during the late-season for pollinators in a dryland, agrivoltaic ecosystem. *Scientific Reports*, *11*(1), 7452. https://doi.org/10.1038/s41598-021-86756-4

Grassi, G., Ripullone, F., Borghetti, M., Raddi, S., & Magnani, F. (2009). Contribution of diffusional and non-diffusional limitations to midday depression of photosynthesis in *Arbutus unedo* L. *Trees*, *23*, 1149–1161. https://doi.org/10.1007/s00468-009-0355-7

Grassroots Ecology. (2022). July native plant of the month: California phacelia. Grassroots Ecology. https://www.grassrootsecology.org/from-the-field/2022/7/14/july-native-plant-of-the-month-california-phacelia

Grossiord, C., Buckley, T. N., Cernusak, L. A., Novick, K. A., Poulter, B., Siegwolf, R. T., Siegwolf, R. T. W., Sperry, J. S., & McDowell, N. G. (2020). Plant responses to rising vapor pressure deficit. *New Phytologist*, *226*(6), 1550–1566. https://doi.org/10.1111/nph.16485

Grossiord, C., Sevanto, S., Limousin, J. M., Meir, P., Mencuccini, M., Pangle, R. E., Pockman, W. T., Salmon, Y., Zweifel, R., & McDowell, N. G. (2018). Manipulative experiments demonstrate how long-term soil moisture changes alter controls of plant water use. *Environmental and Experimental Botany*, *152*, 19–27. https://doi.org/10.1016/j.envexpbot.2017.12.010

Halbritter, A. H., de, H., Eycott, A. E., Reinsch, S., Robinson, D. A., Vicca, S., Berauer, B., Christiansen, C., Estiarte, M., Grünzweig, J., Gya, R., Hansen, K., Jentsch, A., Lee, H., Linder, S., Marshall, J., Peñuelas, J., Kappel, I., Stuart-Haëntjens, E., & Wilfahrt, P. (2020). The handbook for standardized field and laboratory measurements in terrestrial climate change experiments and observational studies (ClimEx). *Methods in Ecology and Evolution*, *11*(1), 22–37.

Hartig, F., & Lohse, L. (2022). Package 'DHARMa': Residual diagnostics for hierarchical (multi-level/mixed) regression models. R package version 0.4, 6.

Hassanpour Adeh, E., Selker, J. S., & Higgins, C. W. (2018). Remarkable agrivoltaic influence on soil moisture, micrometeorology and water-use efficiency. *PLoS ONE*, *13*(11), e0203256. https://doi.org/10.1371/journal.pone.0203256

Hatier, J.-H. B., & Gould, K. S. (2009). Anthocyanin function in vegetative organs. In K. S. Gould, K. M. Davies, & C. Winefield (Eds.), *Anthocyanins: Biosynthesis, functions, and applications* (pp. 1–19). Springer.

Hernandez, R. R., Armstrong, A., Burney, J., Ryan, G., Moore-O'Leary, K., Diédhiou, I., Grodsky, S., Saul-Gershenz, L., Davis, R., Macknick, J., Mulvaney, D., Heath, G., Easter, S., Hoffacker, M., Allen, M., & Kammen, D. (2019). Techno–ecological synergies of solar energy for global sustainability. *Nature Sustainability*, *2*(7), 560–568.

Hernandez, R. R., Patten, T., Li, Y., Levin, M., Condon, D., Krasner, N. Z., & Finkelor, B. (2024). Defining voltaic landscapes for sustainability: Agrivoltaic, rangevoltaic, and ecovoltaic systems. Wild Energy Center - Energy and Efficiency Institute, University of California,Davis. WEC-EEI-000-001

Hughes, N. M. (2011). Winter leaf reddening in 'evergreen' species. *New Phytologist*, *190*(3), 573–581. https://doi.org/10.1111/j.1469-8137.2011.03662.x

Idris, A., Linatoc, A. C., Aliyu, A. M., Muhammad, S. M., & Bakar, M. F. B. A. (2018). Effect of light on the photosynthesis, pigment content and stomatal density of sun and shade leaves of *Vernonia amygdalina*. *International Journal of Engineering & Technology*, *7*(4.30), 209–212. https://doi.org/10.14419/ijet.v7i4.30.22122

IEA. (2024). Renewables 2023, IEA, Paris https://www.iea.org/reports/renewables-2023, Licence: CC BY 4.

Jagodziński, A. M., Dyderski, M. K., Rawlik, K., & Kątna, B. (2016). Seasonal variability of biomass, total leaf area and specific leaf area of forest understory herbs reflects their life strategies. *Forest Ecology and Management*, *374*, 71–81. https://doi.org/10.1016/j.foreco.2016.04.050

Jones, H. G. (1999). Use of infrared thermometry for estimation of stomatal conductance as a possible aid to irrigation scheduling. *Agricultural and Forest Meteorology*, *95*(3), 139–149. https://doi.org/10.1016/S0168-1923(99)00030-1

Kannenberg, S. A., Sturchio, M. A., Venturas, M. D., & Knapp, A. K. (2023). Grassland carbon-water cycling is minimally impacted by a photovoltaic array. *Communications Earth & Environment*, *4*(1), 238. https://doi.org/10.1038/s43247-023-00904-4

Klein, T. (2014). The variability of stomatal sensitivity to leaf water potential across tree species indicates a continuum between isohydric and anisohydric behaviors. *Functional Ecology*, *28*(6), 1313–1320. https://doi.org/10.1111/1365-2435.12289

Knapp, A. K., & Sturchio, M. A. (2024). Ecovoltaics in an increasingly water-limited world: An ecological perspective. *One Earth*, *7*(10), 1705–1712. https://doi.org/10.1016/j.oneear.2024.09.003

Lambers, H., Chapin, F. S., & Pons, T. L. (2008). *Plant physiological ecology* (2nd ed.). Springer.

Lambert, Q., Bischoff, A., Cueff, S., Cluchier, A., & Gros, R. (2021). Effects of solar park construction and solar panels on soil quality, microclimate, CO_2 effluxes, and vegetation under a Mediterranean climate. *Land Degradation & Development*, *32*(18), 5190–5202. https://doi.org/10.1002/ldr.4101

Lambert, Q., Gros, R., & Bischoff, A. (2022). Ecological restoration of solar park plant communities and the effect of solar panels. *Ecological Engineering*, *182*, 106722. https://doi.org/10.1016/j.ecoleng.2022.106722

Lenth, R., & Lenth, M. R. (2018). Package 'lsmeans'. *The American Statistician*, *34*(4), 216–221.

Li, Y., Armstrong, A., Simmons, C., Krasner, N. Z., & Hernandez, R. R. (2025). Ecological impacts of single-axis photovoltaic solar energy with periodic mowing on microclimate and vegetation. *Frontiers in Sustainability*, *6*, 1497256. https://doi.org/10.3389/frsus.2025.1497256

Lichtenthaler, H. K., Ač, A., Marek, M. V., Kalina, J., & Urban, O. (2007). Differences in pigment composition, photosynthetic rates and chlorophyll fluorescence images of sun and shade leaves of four tree species. *Plant Physiology and Biochemistry*, *45*(8), 577–588. https://doi.org/10.1016/j.plaphy.2007.04.006

Lim, S., & Kim, J. (2021). Light quality affects water use of sweet basil by changing its stomatal development. *Agronomy*, *11*(2), 303. https://doi.org/10.3390/agronomy11020303

Liu, Y., Zhang, R. Q., Huang, Z., Cheng, Z., López-Vicente, M., Ma, X. R., & Wu, G. L. (2019). Solar photovoltaic panels significantly promote vegetation recovery by modifying the soil surface microhabitats in an arid sandy ecosystem. *Land Degradation & Development*, *30*(18), 2177–2186. https://doi.org/10.1002/ldr.3408

Maes, W. H., & Steppe, K. (2012). Estimating evapotranspiration and drought stress with ground-based thermal remote sensing in agriculture: A review. *Journal of Experimental Botany*, *63*(13), 4671–4712. https://doi.org/10.1093/jxb/ers165

Magney, T. S., Barnes, M. L., & Yang, X. (2020). On the covariation of chlorophyll fluorescence and photosynthesis across scales. *Geophysical Research Letters*, *47*(23), e2020GL091098. https://doi.org/10.1029/2020GL091098

Mahanty, D. S. (2023). Physiology of shade loving plants: A comparative analysis with shade avoiding plants. *Indian Journal of Applied and Pure Biology*, *38*, 536–546.

Mänd, P., Hallik, L., Peñuelas, J., Nilson, T., Duce, P., Emmett, B. A., Beier, C., Estiarte, M., Garadnai, J., Kalapos, T., Schmidt, I. K., Kovács-Láng, E., Prieto, P., Tietema, A., Westerveld, J. W., & Kull, O. (2010). Responses of the reflectance indices PRI and NDVI to experimental warming and drought in European shrublands along a north–south climatic gradient. *Remote Sensing of Environment*, *114*(3), 626–636. https://doi.org/10.1016/j.rse.2009.11.003

Marrou, H., Dufour, L., & Wery, J. (2013). How does a shelter of solar panels influence water flows in a soil–crop system? *European Journal of Agronomy*, *50*, 38–51. https://doi.org/10.1016/j.eja.2013.05.004

Martin, D. M. (2017). Ecological restoration should be redefined for the twenty-first century. *Restoration Ecology*, *25*(5), 668–673. https://doi.org/10.1111/rec.12554

Mathur, S., Jain, L., & Jajoo, A. (2018). Photosynthetic efficiency in sun and shade plants. *Photosynthetica*, *56*, 354–365. https://doi.org/10.1007/s11099-018-0767-y

McDowell, N., Pockman, W. T., Allen, C. D., Breshears, D. D., Cobb, N., Kolb, T., Plaut, J., Sperry, J., West, A., Williams, D. G., & Yepez, E. A. (2008). Mechanisms of plant survival and mortality during drought: Why do some plants survive while others succumb to drought? *New Phytologist*, *178*(4), 719–739. https://doi.org/10.1111/j.1469-8137.2008.02436.x

Merzlyak, M. N., Chivkunova, O. B., Solovchenko, A. E., & Naqvi, K. R. (2008). Light absorption by anthocyanins in juvenile, stressed, and senescing leaves. *Journal of Experimental Botany*, *59*(14), 3903–3911. https://doi.org/10.1093/jxb/ern230

Michaletz, S. T., Weiser, M. D., McDowell, N. G., Zhou, J., Kaspari, M., Helliker, B. R., & Enquist, B. J. (2016). The energetic and carbon economic origins of leaf thermoregulation. *Nature Plants*, *2*(9), 1–9.

Narayanan, S., Prasad, P. V. V., Fritz, A. K., Boyle, D. L., & Gill, B. S. (2015). Impact of high night-time and high daytime temperature stress on winter wheat. *Journal of Agronomy and Crop Science*, *201*(3), 206–218. https://doi.org/10.1111/jac.12101

Niinemets, Ü. (2010). Responses of forest trees to single and multiple environmental stresses from seedlings to mature plants: Past stress history, stress interactions, tolerance and acclimation. *Forest Ecology and Management*, *260*(10), 1623–1639. https://doi.org/10.1016/j.foreco.2010.07.054

Plants For A Future. (2025). Grindelia camporum. Retrieved March 6, 2025, from https://pfaf.org/user/Plant.aspx?LatinName=Grindelia+camporum

Pompodakis, N. E., Terry, L. A., Joyce, D. C., Lydakis, D. E., & Papadimitriou, M. D. (2005). Effect of seasonal variation and storage temperature on leaf chlorophyll fluorescence and vase life of cut roses. *Postharvest Biology and Technology*, *36*(1), 1–8. https://doi.org/10.1016/j.postharvbio.2004.11.003

Poorter, H., Niinemets, Ü., Ntagkas, N., Siebenkäs, A., Mäenpää, M., Matsubara, S., & Pons, T. (2019). A meta-analysis of plant responses to light intensity for 70 traits ranging from molecules to whole plant performance. *New Phytologist*, *223*(3), 1073–1105. https://doi.org/10.1111/nph.15754

Poorter, H., Niinemets, Ü., Poorter, L., Wright, I. J., & Villar, R. (2009). Causes and consequences of variation in leaf mass per area (LMA): A meta-analysis. *New Phytologist*, *182*(3), 565–588. https://doi.org/10.1111/j.1469-8137.2009.02830.x

Putah Creek Council. (2025). Great Valley gumweed (Grindelia camporum). Retrieved March 6, 2025, from https://putahcreekcouncil.org/creekside-neighbors/great-valley-gumweed-grindelia-camporum

Rinza, J., Ramírez, D., & Ninanya, J. (2021). Practical field guide. Functional crop monitoring for early stress detection: Stomatal conductance and infrared thermography as key measurement tools. Retrieved July

24, 2022, from https://cgspace.cgiar.org/items/f3a4b27c-b809-4f8e-91a4-13b371d946db

Schneider, C. A., Rasband, W. S., & Eliceiri, K. W. (2012). NIH image to ImageJ: 25 years of image analysis. *Nature Methods*, *9*(7), 671–675. https://doi.org/10.1038/nmeth.2089

Semeraro, T., Scarano, A., Curci, L. M., Leggieri, A., Lenucci, M., Basset, A., Santino, A., Piro, G., & De Caroli, M. (2024). Shading effects in agrivoltaic systems can make the difference in boosting food security in climate change. *Applied Energy*, *358*, 122565. https://doi.org/10.1016/j.apenergy.2023.122565

Serbin, S. P., Singh, A., Desai, A. R., Dubois, S. G., Jablonski, A. D., Kingdon, C. C., … Townsend, P. A. (2015). Remotely estimating photosynthetic capacity, and its response to temperature, in vegetation with hyperspectral spectroscopy. *New Phytologist*, *205*(1), 279–301.

SoilWeb. (2024). Soil survey information from the USDA-NRCS. University of California, Davis. Retrieved from https://casoilresource.lawr.ucdavis.edu/soilweb-apps/

Sperry, J. S., & Love, D. M. (2015). What plant hydraulics can tell us about responses to climate-change droughts. *New Phytologist*, *207*(1), 14–27. https://doi.org/10.1111/nph.13354

Sturchio, M. A., Kannenberg, S. A., Pinkowitz, T. A., & Knapp, A. K. (2024). Solar arrays create novel environments that uniquely alter plant responses. *Plants, People, Planet*, *6*, 1522–1533. https://doi.org/10.1002/ppp3.10554

Sturchio, M. A., & Knapp, A. K. (2023). Ecovoltaic principles for a more sustainable, ecologically informed solar energy future. *Nature Ecology & Evolution*, *7*(11), 1746–1749. https://doi.org/10.1038/s41559-023-02174-x

Sturchio, M. A., Macknick, J. E., Barron-Gafford, G. A., Chen, A., Alderfer, C., Condon, K., Hajek, O. L., Miller, B., Pauletto, B., Siggers, J. A., Slette, I. J., & Knapp, A. K. (2022). Grassland productivity responds unexpectedly to dynamic light and soil water environments induced by photovoltaic arrays. *Ecosphere*, *13*(12), e4334. https://doi.org/10.1002/ecs2.4334

Suuronen, A., Muñoz-Escobar, C., Lensu, A., Kuitunen, M., Guajardo Celis, N., Espinoza Astudillo, P., Ferrú, M., Taucare-Ríos, A., Miranda, M., Kukkonen, J. V. K., & Kukkonen, J. V. (2017). The influence of solar power plants on microclimatic conditions and the biotic community in Chilean desert environments. *Environmental Management*, *60*(4), 630–642. https://doi.org/10.1007/s00267-017-0906-4

Tanner, K. E., Moore-O'Leary, K. A., Parker, I. M., Pavlik, B. M., Haji, S., & Hernandez, R. R. (2021). Microhabitats associated with solar energy development alter demography of two desert annuals. *Ecological Applications*, *31*(6), e02349.

Tanner, K. E., Moore-O'Leary, K. A., Parker, I. M., Pavlik, B. M., & Hernandez, R. R. (2020). Simulated solar panels create altered microhabitats in desert landforms. *Ecosphere*, *11*(4), e03089. https://doi.org/10.1002/ecs2.3089

Tölgyesi, C., Bátori, Z., Pascarella, J., Erdős, L., Török, P., Batáry, P., & Gallé, R. (2023). Ecovoltaics: Framework and future research directions to reconcile land-based solar power development with ecosystem conservation. *Biological Conservation*, *285*, 110242. https://doi.org/10.1016/j.biocon.2023.110242

Tsukaya, H. (2013). Leaf development. *The Arabidopsis Book*, *11*, e0163. https://doi.org/10.1199/tab.0163

U.S. Climate Data. (2024). Climate data for the United States. Retrieved September 23, 2024, from https://www.usclimatedata.com

Uldrijan, D., Černý, M., & Winkler, J. (2022). Solar park: Opportunity or threat for vegetation and ecosystem. *Journal of Ecological Engineering*, *23*(11), 1–10. https://doi.org/10.12911/22998993/153456

Uldrijan, D., Kováčiková, M., Jakimiuk, A., Vaverková, M. D., & Winkler, J. (2021). Ecological effects of preferential vegetation composition developed on sites with photovoltaic power plants. *Ecological Engineering*, *168*, 106274. https://doi.org/10.1016/j.ecoleng.2021.106274

Urban, J., Ingwers, M. W., McGuire, M. A., & Teskey, R. O. (2017). Increase in leaf temperature opens stomata and decouples net photosynthesis from stomatal conductance in Pinus taeda and Populus deltoides x nigra. *Journal of Experimental Botany*, *68*(7), 1757–1767. https://doi.org/10.1093/jxb/erx052

Valladares, F., & Niinemets, Ü. (2008). Shade tolerance, a key plant feature of complex nature and consequences. *Annual Review of Ecology, Evolution, and Systematics*, *39*, 237–257. https://doi.org/10.1146/annurev.ecolsys.39.110707.173506

Vaverková, M. D., Winkler, J., Uldrijan, D., Ogrodnik, P., Vespalcová, T., Aleksiejuk-Gawron, J., Adamcová, D., & Koda, E. (2022). Fire hazard associated with different types of photovoltaic power plants: Effect of vegetation management. *Renewable and Sustainable Energy Reviews*, *162*, 112491. https://doi.org/10.1016/j.rser.2022.112491

Walston, L. J., Hartmann, H. M., Fox, L., Macknick, J., McCall, J., Janski, J., & Jenkins, L. (2023). If you build it, will they come? Insect community responses to habitat establishment at solar energy facilities in Minnesota, USA. *Environmental Research Letters*, *19*(1), 014053. https://doi.org/10.1088/1748-9326/ad0f72

Walston, L. J., Li, Y., Hartmann, H. M., Macknick, J., Hanson, A., Nootenboom, C., Lonsdorf, E., & Hellmann, J. (2021). Modeling the ecosystem services of native vegetation management practices at solar energy facilities in the Midwestern United States. *Ecosystem Services*, *47*, 101227. https://doi.org/10.1016/j.ecoser.2020.101227

Walston, L. J., Mishra, S. K., Hartmann, H. M., Hlohowskyj, I., McCall, J., & Macknick, J. (2018). Examining the potential for agricultural benefits from pollinator habitat at solar facilities in the United States. *Environmental Science & Technology*, *52*(13), 7566–7576. https://doi.org/10.1021/acs.est.8b00020

Wang, Q. W., Robson, T. M., Pieristè, M., Oguro, M., Oguchi, R., Murai, Y., & Kurokawa, H. (2020). Testing trait plasticity over the range of spectral composition of sunlight in forb species differing in shade tolerance. *Journal of Ecology*, *108*(5), 1923–1940. https://doi.org/10.1111/1365-2745.13384

Wang, Y., Chen, Y., Zhang, X., & Gong, W. (2021). Research on measurement method of leaf length and width based on point cloud. *Agriculture*, *11*(1), 63. https://doi.org/10.3390/agriculture11010063

Ward, A. D., & Trimble, S. W. (2003). *Environmental hydrology*. Crc Press.

Wu, C., Liu, H., Yu, Y., Zhao, W., Liu, J., Yu, H., & Yetemen, O. (2022). Eco-hydrological effects of photovoltaic solar farms on soil microclimates and moisture regimes in arid Northwest China: A modeling study. *Science of the Total Environment*, *802*, 149946. https://doi.org/10.1016/j.scitotenv.2021.149946

Wynne-Sison, T., Devitt, D. A., & Smith, S. D. (2023). Ecovoltaics: Maintaining native plants and wash connectivity inside a Mojave Desert solar facility leads to favorable growing conditions. *Land*, *12*(10), 1950. https://doi.org/10.3390/land12101950

Yue, S., Guo, M., Zou, P., Wu, W., & Zhou, X. (2021). Effects of photovoltaic panels on soil temperature and moisture in desert areas. *Environmental Science and Pollution Research*, *28*, 11751–17506.

SUPPORTING INFORMATION

Additional supporting information can be found online in the Supporting Information section at the end of this article.

How to cite this article: Li, Y., Magney, T., Armstrong, A., & Hernandez, R. R. (2025). Made in the shade: Leaf responses of native wildflowers to single-axis photovoltaic solar energy. *Plants, People, Planet*, 1–17. https://doi.org/10.1002/ppp3.70138